

UNIVERSITY OF BIRMINGHAM

University of Birmingham
Research at Birmingham

Experimental investigation of particle emissions from a Dieseline fuelled compression ignition engine

Zeraati-Rezaei, Soheil; Al-Qahtani, Yasser; Herreros, Jose M.; Ma, Xiao; Xu, Hongming

DOI:

[10.1016/j.fuel.2019.03.138](https://doi.org/10.1016/j.fuel.2019.03.138)

License:

Creative Commons: Attribution-NonCommercial-NoDerivs (CC BY-NC-ND)

Document Version

Peer reviewed version

Citation for published version (Harvard):

Zeraati-Rezaei, S, Al-Qahtani, Y, Herreros, JM, Ma, X & Xu, H 2019, 'Experimental investigation of particle emissions from a Dieseline fuelled compression ignition engine', *Fuel*, vol. 251, pp. 175-186.
<https://doi.org/10.1016/j.fuel.2019.03.138>

[Link to publication on Research at Birmingham portal](#)

General rights

Unless a licence is specified above, all rights (including copyright and moral rights) in this document are retained by the authors and/or the copyright holders. The express permission of the copyright holder must be obtained for any use of this material other than for purposes permitted by law.

- Users may freely distribute the URL that is used to identify this publication.
- Users may download and/or print one copy of the publication from the University of Birmingham research portal for the purpose of private study or non-commercial research.
- User may use extracts from the document in line with the concept of 'fair dealing' under the Copyright, Designs and Patents Act 1988 (?)
- Users may not further distribute the material nor use it for the purposes of commercial gain.

Where a licence is displayed above, please note the terms and conditions of the licence govern your use of this document.

When citing, please reference the published version.

Take down policy

While the University of Birmingham exercises care and attention in making items available there are rare occasions when an item has been uploaded in error or has been deemed to be commercially or otherwise sensitive.

If you believe that this is the case for this document, please contact UBIRA@lists.bham.ac.uk providing details and we will remove access to the work immediately and investigate.

1 **Experimental Investigation of Particle Emissions from a Dieseline**

2 **Fuelled Compression Ignition Engine**

3 Soheil ZERAATI-REZAEI ^a, Yasser AL-QAHTANI ^a, Jose M. HERREROS ^a, Xiao MA ^b
4 and Hongming XU ^{a, b} *

5 ^aDepartment of Mechanical Engineering, University of Birmingham, Birmingham B15 2TT, UK.

6 ^bState Key Laboratory of Automotive Safety and Energy, Tsinghua University, Beijing 100084, China.

7 * Corresponding author. Telephone: +44 (0) 121 414 4153, Email: h.m.xu@bham.ac.uk

8 **ABSTRACT**

9 Achieving low-smoke and low-NO_x premixed compression ignition (PCI) combustion at a
10 wide engine operating load range has been a challenge; especially in multi-cylinder engines
11 running at higher loads for which less data is available in the literature. More specifically, it is
12 of interest to characterise particle emissions under these conditions and identify their possible
13 reduction benefit in different size classes compared to conventional diesel combustion. Mixing
14 diesel with gasoline (Dieseline) as an incentive to reduce fuel reactivity (cetane-number) and
15 consequently improve premixing is believed to be useful for PCI. In this study, the feasibility
16 and benefits of using low cetane-number (<30) and wide boiling range G75-Dieseline (75%
17 gasoline in diesel based on volume) in a production light-duty 4-cylinder CI engine are
18 investigated at medium-high loads of 6, 12 and 17.3 bar BMEP. It was found that G75
19 combustion resulted in lower particle emissions (both number and mass), by up to 99.5%, while
20 maintaining the same range of efficiency and NO_x compared to diesel combustion. Bimodal
21 particle size distributions were observed for both G75 and diesel while concentrations of G75
22 particles were much lower across the entire diameter range. For G75, increase of fuel injection
23 pressure decreased particle number concentration (especially in nucleation mode) while
24 particle mass was less affected. At medium loads, because of longer ignition-dwell of G75

25 compared to diesel, variations of combustion and emission characteristics were more sensitive
26 to injection timing. At high loads, mixing-controlled combustion phase was observed for G75
27 and highlighted the importance of investigating advanced intake pressure boosting systems and
28 interactions between fuel spray and piston.

29 **Keywords:** PCI; Dieseline; Low cetane, Injection strategy; Particulate matter; NO_x

30

31 1 INTRODUCTION

32 Using premixed compression ignition (PCI) combustion techniques can effectively decrease
33 engine-out soot and oxides of nitrogen (NO_x) emissions compared to conventional diesel CI
34 [1-7]. This is normally achieved by using longer fuel ignition-delay (enhanced local premixing)
35 and higher exhaust gas recirculation (lower intake O_2 concentration and local combustion
36 temperature) [7]. Generally, engine operating range is a challenge to overcome when using PCI
37 techniques as they are normally limited to low, not very low though, and medium loads. At
38 higher loads, the global and local equivalence ratios are closer to stoichiometric strength and
39 auto-ignition of multiple points happens more rapidly leading to high peak heat release rates,
40 pressure rise rates, NO_x and possibly particle emissions [1, 8]. Low auto-ignition tendency (low
41 cetane-number (CN) or long ignition-delay (ID) or low reactivity) and high volatility of the
42 fuel can help achieve the objectives of PCI type combustion in a wider load range [1].

43 Results from the recent research in the area of PCI suggest usage of a gasoline-like fuel with a
44 research octane number (RON) between 70 and 85 [1, 9]. Among the readily available options,
45 mixing of diesel with gasoline (named as Dieseline) seems to be a very promising choice to
46 increase the reactivity of high RON conventional gasoline fuel. Using Dieseline has been
47 proven to enhance the PCI combustion at low-medium loads and is being considered as one of
48 the fuel candidates for the future use (e.g. [5, 6, 10-16]). Various gasoline volumetric blend-
49 ratios in the Dieseline fuel has been studied for PCI at low-medium loads, e.g. between 0% and
50 75% (G0-Dieseline and G75-Dieseline) [5-7, 12, 13, 17]. These studies showed that smoke and
51 NO_x emissions were reduced, by up to 99% compared to neat diesel combustion, especially for
52 the case of G75-Dieseline (G75) [7] that has an estimated RON of approximately 75 and
53 consequently long ID. In addition to these studies at low-medium loads, possible application
54 of the Dieseline PCI technique in multi-cylinder engines requires investigating combustion
55 performance and emissions characteristics at higher loads. It is particularly important to

56 evaluate the reduction of particles compared to diesel combustion and its impact on engine
57 efficiency and NO_x emissions.

58 A few studies are available on the particle emissions from CI engines using fuels that contain
59 only small to moderate (not high) gasoline blend-ratios in Dieseline at medium-high engine
60 loads (e.g. [18-21]). Wei *et al.* [18] studied a maximum gasoline blend ratio of 30% at a
61 maximum brake mean effective pressure (BMEP) of 11.3 bar without any exhaust gas
62 recirculation (EGR) in a light/medium-duty CI engine. They concluded that total concentration
63 of particles with smaller diameters (mainly in the nucleation mode) was generally higher than
64 the case of diesel combustion. Belgiorno *et al.* [19] investigated the mixtures of diesel, gasoline
65 and ethanol (with a maximum gasoline+ethanol ratio of 44%) in a single-cylinder CI engine at
66 a maximum load of 13 bar BMEP. They reported that nucleation mode particles were higher
67 than diesel in lower loads while accumulation mode particles were higher at higher loads.
68 Benajes *et al.* [20, 21] investigated dual-mode/dual-fuel (combining reactivity controlled CI
69 (RCCI [22]) and diffusive combustion) in a single-cylinder medium-duty CI engine at a
70 maximum load of 22 and 23 bar indicated MEP for which gasoline ratio in Dieseline was 34%
71 and 32%. Total particle number results were higher than conventional diesel combustion.
72 Although gasoline blend-ratio was different for different loads, they concluded that nucleation
73 mode particles and accumulation mode particles were higher in lower and higher loads,
74 respectively.

75 The results from these recent studies motivated the current research into particle emissions
76 from combustion of Dieseline with higher blend-ratios of gasoline at medium-high engine
77 loads especially in multi-cylinder CI engines. It is of interest to characterise particle emissions
78 and identify their possible reduction in all size classes.

79 In the current paper, PCI combustion of G75-Dieseline is evaluated in terms of efficiency and
80 emissions. Different fuel injection pressures and timings with various EGR options are
81 investigated in a production light-duty multi-cylinder diesel engine at loads of 6, 12 and 17.3
82 bar BMEP. The experimental setup is described in the next section and is followed by the
83 comparison and discussion of G75 combustion and diesel combustion results. A summary and
84 conclusions of this paper are provided at the end.

85 **2 EXPERIMENTAL SETUP**

86 Experiments were carried out on a production 2.2 L, 4-cylinder in-line compression ignition
87 (CI) engine. It is equipped with a variable-nozzle-turbine (VNT) turbocharger and a common
88 rail direct-injection (DI) system. Major engine specifications are provided in Table 1 and a
89 schematic of the engine test cell is shown in Figure 1; further details are described in [7]. In
90 this paper, hot-EGR means that the EGR cooler and air intercooler are either completely or
91 partially deactivated by means of the valves illustrated in Figure 1. Cold-EGR term is used
92 when full cooling intensity of the EGR cooler and the air intercooler are used.

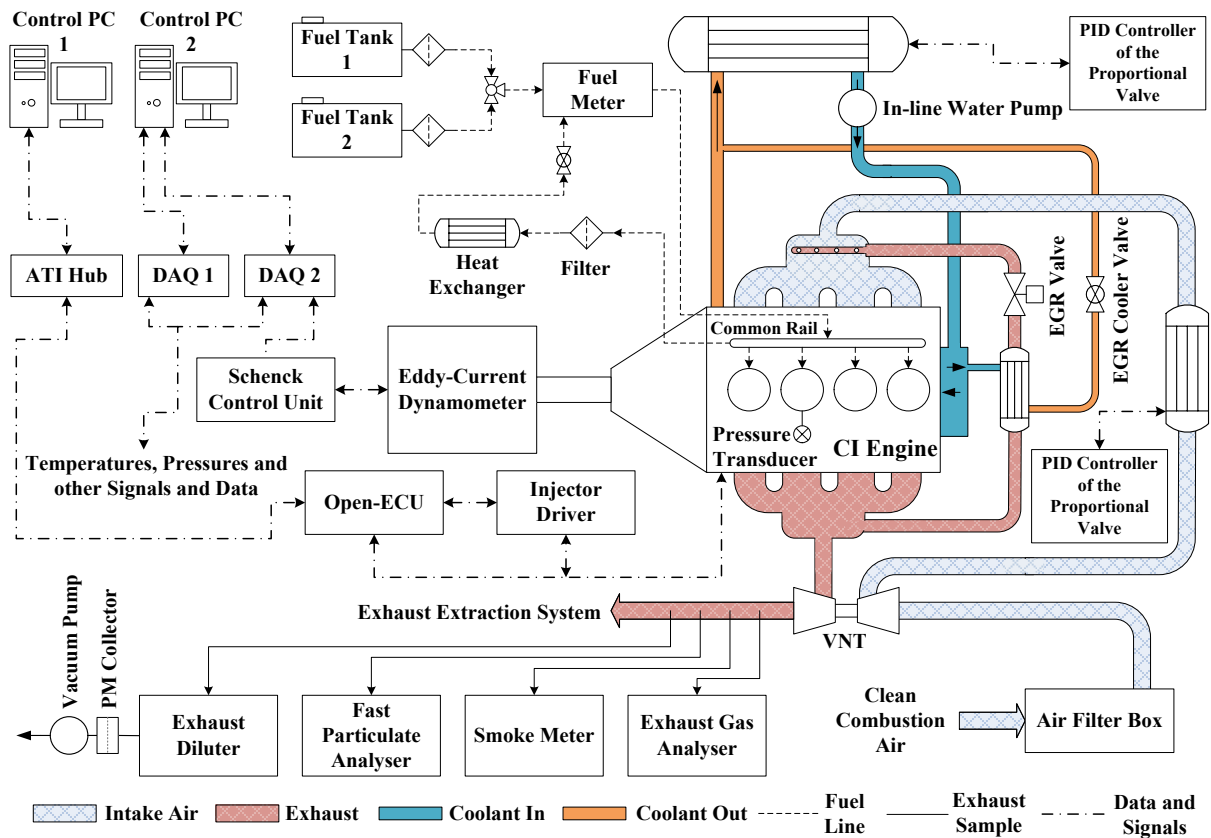
93

94

Table 1 Engine specifications

Bore (mm)	86.0
Stroke (mm)	94.6
Connecting Rod Length (mm)	155.0
Displacement (cm³)	2198
Compression Ratio	15.5:1
Injection System	DI Common Rail
Injectors	Solenoid, 7 Holes (0.15mm diameter)

95



96

97

Figure 1 Schematic of the engine test cell

98

99 A Pi-Innovo M250 open engine control unit (Open-ECU) is utilised in this test cell and allows
 100 flexible control over the engine operating settings, e.g. injection events, EGR valve, VNT
 101 actuator, etc. Fuel injection-timing (IT) is obtained from the Open-ECU which indicates the
 102 start of the energising.

103 The clean combustion air shown in Figure 1 is from the lab air supply system and its
 104 temperature was fixed at 22 ± 1 °C. Temperature of the engine coolant out was controlled to be
 105 90 ± 1 °C. K-type thermocouples were used to measure temperature at different locations and at
 106 each test point, data were averaged for 180 s.

107 In-cylinder pressure of the engine was measured with a calibrated Kistler 6058A non-cooled
 108 piezo star pressure transducer (linearity $\leq \pm 0.05\%$ of the full scale output) equipped with a

109 Kistler 6544Q192 glow-plug adaptor and a Kistler 5011B10Y50 charge amplifier (linearity \leq
110 $\pm 0.05\%$). An AMI-Elektronik/Art.No:41500043-00360 shaft encoder was used and in-cylinder
111 pressure data were logged at each crank angle degree (CAD) for 200 engine operating cycles.
112 These data were used to calculate some of the combustion related parameters, e.g. apparent net
113 heat release rate [7, 23].

114 Start of combustion (SOC) is the CAD at which heat release rate curve passes the zero level
115 from a negative value to a positive value after the start of fuel injection. Ignition-delay (ID) is
116 the CAD duration from the start of injection-timing to the SOC. Combustion-phasing or AHR-
117 50 is defined as the CAD at which 50% of the accumulative heat release is achieved. Ignition-
118 dwell is defined as the CAD duration from the end of injection (EOI) to the SOC.

119 Fuel consumption was measured and averaged over 180 s using a frequently calibrated AVL
120 733s dynamic fuel meter (error between 0.12% and 0.2%) equipped with an AVL 752-60 fuel
121 cooler. A Horiba MEXA-7100-DEGR exhaust gas analyser (measurement linearity $\leq \pm 1\%$ of
122 the full scale output) was used to measure gaseous emissions and data were averaged over 180
123 s. CO₂ concentrations in the intake manifold (after the entry of the EGR tube) and exhaust were
124 used to calculate the EGR percentage. Smoke emissions were measured using an AVL smoke
125 meter (model 415S). In terms of repeatability, the standard deviation (SD) of the measurements
126 by the smoke meter is $< \pm 0.005 \text{ FSN} + 3\%$ of the measured value.

127 A calibrated fast particulate analyser from Cambustion (DMS500 MKII) working based on the
128 differential mobility spectroscopy (DMS) principle was used to measure particle emission
129 (from sizes around 5 nm to 1000 nm) from the engine exhaust. It separates different sizes of
130 particles based on their charge and aerodynamic drag while migrating in an electric field [24].
131 Particle size distribution data are averaged over 60 s for a single measurement while each data
132 point presented in this paper is the average of multiple measurements. Total particle number

133 concentrations are derived from integrating the data while nucleation and accumulation mode
134 concentrations are derived from log-normal curve fittings. A software package provided by
135 Cambustion utilising a Bayesian statistical algorithm [25] was used to separate the two
136 aforementioned modes based on the concentration, mean size and width (geometric standard
137 deviation) of the distribution [24]. In this way, total mass can be calculated more accurately,
138 as explained in [26], since the characteristics (e.g. effective density and physical geometry) of
139 particles of each mode are different.

140 The experimental data presented in this paper were collected under the steady-state engine
141 operating conditions and are averages of multiple measurements (at least three) while
142 considering the standard deviation.

143 Specification EN 590 normal European ultra-low sulphur diesel (ULSD) and G75-Dieseline
144 (G75) fuels were used in this study. G75 is a blend of 75% (based on volume) neat normal
145 European RON95 unleaded gasoline (ULG95) (specification EN 228) in the ULSD. To avoid
146 possible failure of the high pressure injection system, ULG95 was enriched with 300
147 volumetric parts per million of the Paradyne R655 fuel lubricity improver. Major available
148 properties of the utilised fuels are provided in Table 2 [7]. The boiling curves of the utilised
149 fuels have been presented elsewhere [7].

150

151

152

153

Table 2 Properties of the utilised fuels [7]

	Diesel	G75-Dieseline	Gasoline
Density at 15 °C (kg/m³)	835.1	768.2	742.8
RON (-)	-	~75*	95.4
MON (-)	-	-	86.6
CN (-)	52.6	-	-
Derived CN (-) [×]	-	30.0	-
Cetane Index (-)	-	27.2	-
Net Calorific Value (MJ/kg)	42.72	42.52	42.34
Total Paraffins (v/v %)	-	57.8	47.1
Olefins (v/v %)	-	7.2	7.9
Naphthenes (v/v %)	-	-	6.3
Aromatics (v/v %)	-	31.7	26

155 * this value is estimated based on the equation provided in [27] considering Cetane Index

156 [×] DCN measurement is certified for 33 < DCN < 64; at DCN= 34, the reproducibility is ±2.21

157 - means the value is not available

158

159 In this paper, G75 and diesel combustion are investigated at the engine loads of 6, 12 and 17.3
 160 bar BMEP and engine speed of 1800 revolutions per minute (RPM) using single-injection. 17.3
 161 bar BMEP is the maximum possible load that can be tested in the current engine test cell.
 162 Screening experiments at loads more than 6 bar BMEP showed that using low IPs (150, 250
 163 and 350 bar) and/or hot-EGR strategy were not suitable for obtaining low smoke and NO_x
 164 emissions from the G75 PCI combustion, as opposed to observations at lower loads [7].
 165 Therefore, higher IPs and cold-EGR strategy were used for all of the tests conducted at these
 166 loads.

167

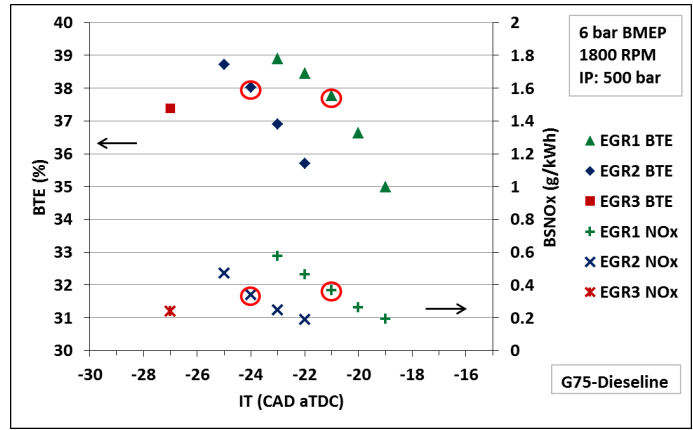
168 3 RESULTS AND DISCUSSION

169 3.1. Results at 6 bar BMEP

170 Figure 2 illustrates brake thermal efficiency (BTE) and brake specific (BS) NO_x results for G75
171 fuel using three IPs, three EGR valve settings (referring to the opening level of the EGR valve)
172 and various ITs. EGR1 refers to 48.5%, EGR 2 refers to 50.5% and EGR3 refers to 52.5%
173 valve opening of the full opening position of the EGR valve. The actuation level of the
174 turbocharger vanes was kept constant for all of these experiments. The reason for selecting this
175 strategy was the fact that maintaining the EGR rate at a fixed level when the IT was being
176 modified was challenging since there is an interaction between the EGR valve and the
177 turbocharger in the multi-cylinder production engine. Therefore, it was decided to maintain
178 valve positions at some defined settings concluded from several screening experiments and this
179 was beneficial for maintaining specific air-fuel ratio (λ) at the desirable levels. With these
180 settings, λ was between 1.2 and 1.4 while λ of EGR1>EGR2>EGR3 at the same combustion-
181 phasing. EGR percentage was between 30% to 34% and engine intake pressure was between
182 1.20 to 1.28 bar absolute. At a fixed EGR valve opening level while using different ITs, EGR
183 percentage variation was generally less than 1% (in absolute value). These strategies were
184 proved to be effective for showing a clear variation trend of engine performance and emission
185 characteristics when using different EGR rates, IPs and ITs. The range of ITs presented in
186 Figure 2 was chosen based on two selected constraints: maximum pressure rise rate
187 (MPRR)<12 bar/CAD and BTE>33%.

188

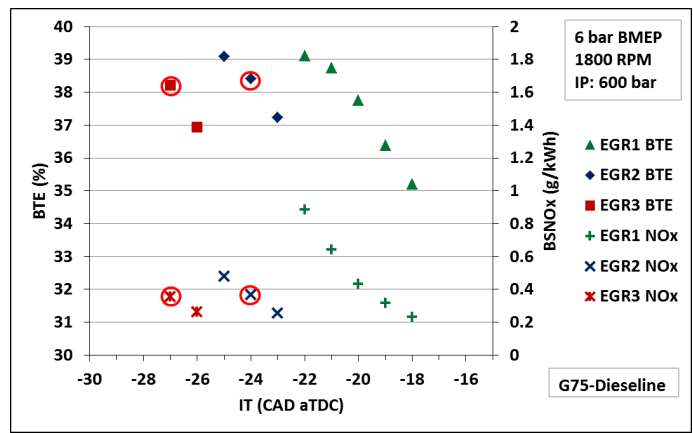
189



190

(a)

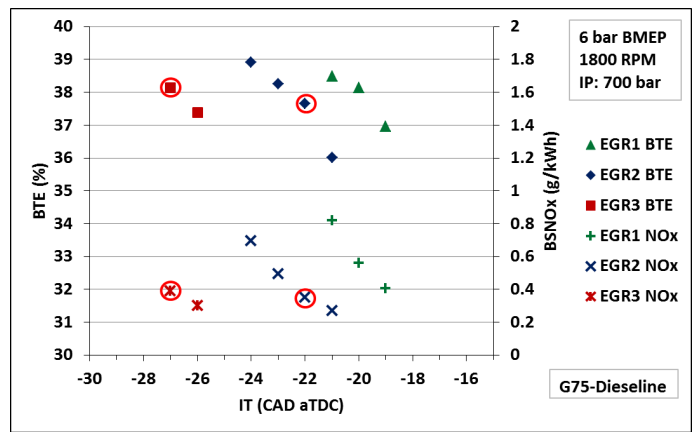
191



192

(b)

193



194

(c)

195

196

197

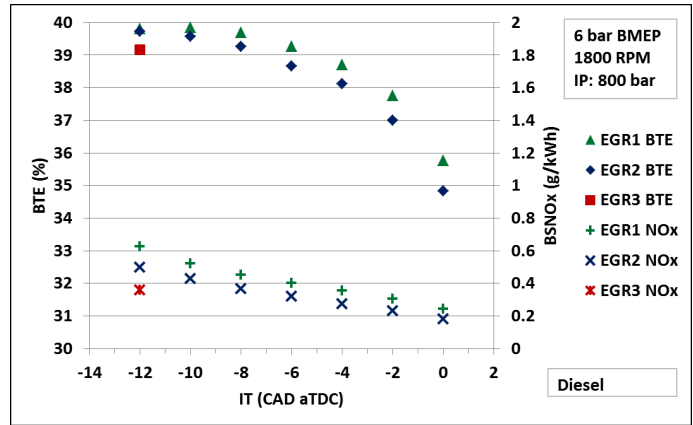
Figure 2 BTE and BSNO_x for G75 with different EGR valve positions and injection-timings with injection pressure of: (a) 500 bar, (b) 600 bar and (c) 700 bar at 6 bar BMEP; red circles in the figure mark the highest achieved BTE while BSNO_x was below 0.4 g/kWh

198 Based on Figure 2, at each IP, BTE and BSNO_x were functions of IT and EGR valve position.
199 Advancing IT increased BTE and BSNO_x emissions. This is because combustion-phasing was
200 advanced as earlier IT was used and therefore more expansion work was drawn from the
201 combusting mixture while in-cylinder temperature at the point of combustion was higher. More
202 opening of the EGR valve helped to achieve more advanced ITs without surpassing the 12
203 bar/CAD constraint for MPRR due to prolonged ignition-delay. With the same IT, increasing
204 EGR valve opening and consequently reducing λ resulted in lower BSNO_x and BTE as
205 expected. This is mainly due to the fact that lower intake O₂ concentration decreases the rate of
206 NO_x production [28] and reduces combustion efficiency. In general, with the same IT and EGR
207 settings, increasing IP resulted in higher values of BSNO_x and BTE as the AHR-50 was being
208 advanced (approached towards the top dead centre (TDC)). A higher IP is associated with
209 shorter injection durations (at a fixed engine load) and can help prepare fuel-air packets which
210 are more readily combustible in a shorter period of time.

211 It can be concluded that there was a trade-off between increasing BTE and reducing NO_x at 6
212 bar BMEP for G75 PCI combustion. This trade-off was not evident in lower engine operating
213 loads [7]. Considering the BSNO_x target value defined arbitrarily to be less than 0.4 g/kWh,
214 within the studied test points when using IP of 600 bar, IT of -24 CAD after TDC (aTDC) and
215 EGR rate of 32.74%, a maximum BTE of 38.41% was achieved and its corresponding BSNO_x
216 value was 0.36 g/kWh.

217 Figure 3 shows BTE and BSNO_x results for diesel with the same EGR valve strategy used for
218 G75 but with different ITs and IPs. Using the same IPs which were used for G75 resulted in
219 high smoke emissions at the same AHR-50 while BSNO_x emissions were around 0.4 g/kWh.
220 Therefore, higher range of IPs were utilised which are normally used in diesel engines for this
221 speed and load [5, 13]. With respect to G75, ITs had to be retarded to avoid high MPRR and
222 intense combustion before the TDC due to the shorter ignition-delay of the diesel fuel.

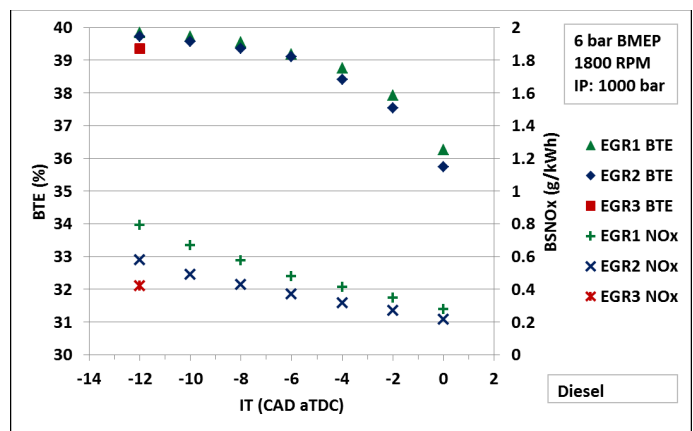
223



224

(a)

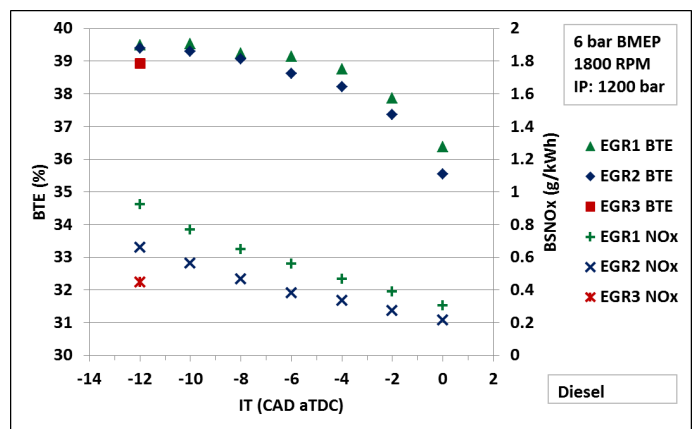
225



226

(b)

227



228

(c)

229

Figure 3 BTE and BSNO_x for diesel with different EGR valve positions and injection-timings with

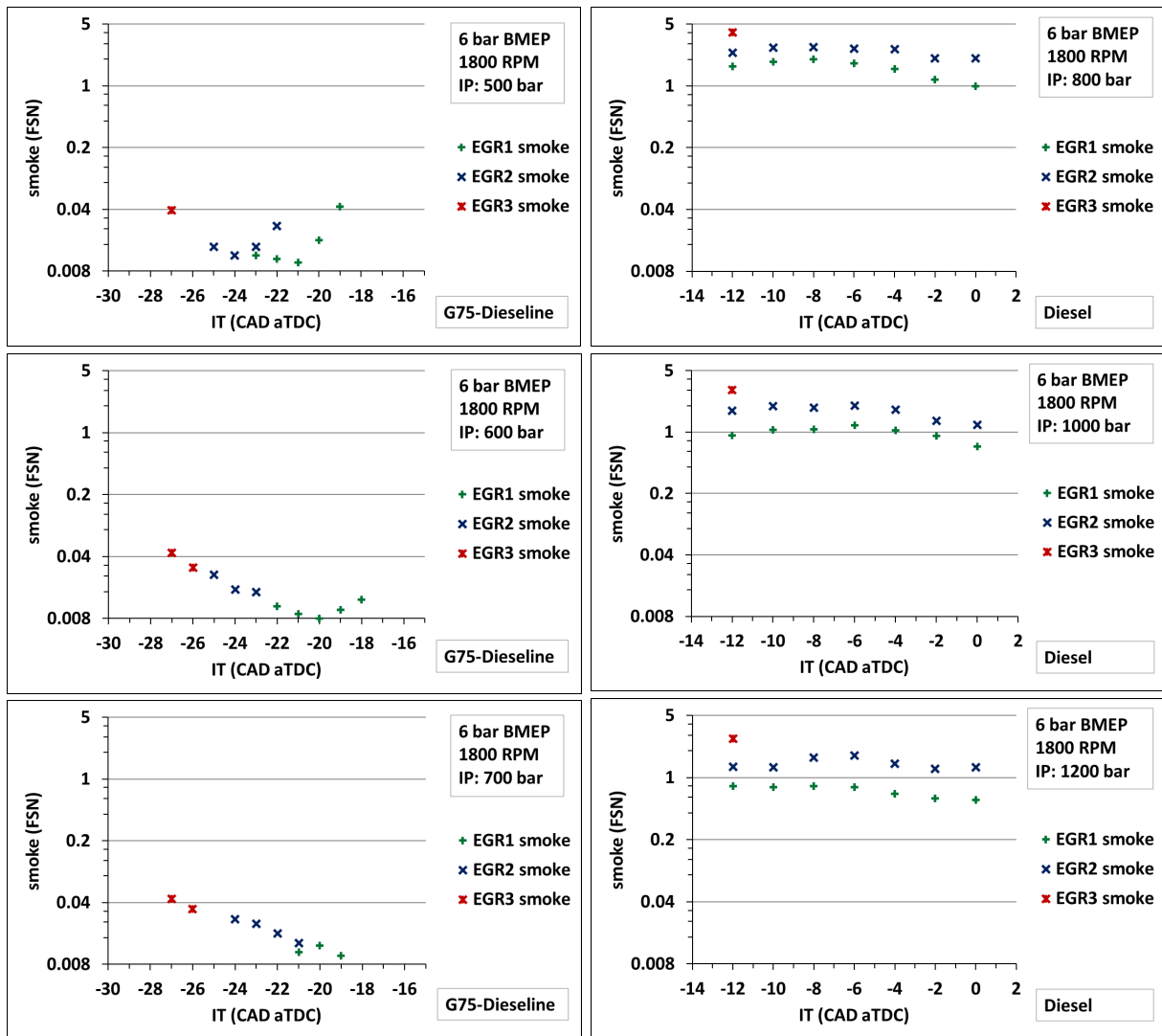
230

injection pressure of: (a) 800 bar, (b) 1000 bar and (c) 1200 bar at 6 bar BMEP

231 Considering the BSNO_x target of <0.4 g/kWh, BTE levels for diesel were in the same range as
232 G75 results (between around 38% to 39%) while smoke emissions were considerably higher
233 (illustrated in Figure 4). Similar to the case of G75, using more advanced ITs resulted in higher
234 BTE and BSNO_x values. Increasing the IP of diesel fuel, from 800 bar to 1200 bar, resulted in
235 an earlier AHR-50 and consequently higher BSNO_x when using a fixed IT and EGR valve
236 opening. For diesel, increasing the IP resulted in higher MPRR which can be linked to the
237 combustion induced noise. These results indicate the effectiveness of AHR-50, λ and IP for
238 controlling combustion and emissions characteristics.

239 Smoke emission results for both G75 and diesel are illustrated in Figure 4. G75 combustion
240 resulted in very low smoke values (mostly below 0.04 FSN) using the studied IPs, ITs and EGR
241 valve openings. Diesel fuel combustion resulted in higher smoke emissions mainly due to its
242 shorter ID and consequently fuel-air mixing time. For diesel, utilising higher IP combined with
243 retarded IT helped to reduce smoke, however smoke emissions never reached below 0.5 FSN.
244 These reductions in FSN were obtained with the lowest studied EGR valve opening (which
245 normally resulted in higher BSNO_x) and retarded IT (which normally resulted in lower BTE).
246 Thus, in the case of diesel combustion at 6 bar BMEP, simultaneous reduction of smoke and
247 NO_x had a drawback of reduced BTE (similar to the observations at 1.4 and 3 bar BMEP [7]).

248



249

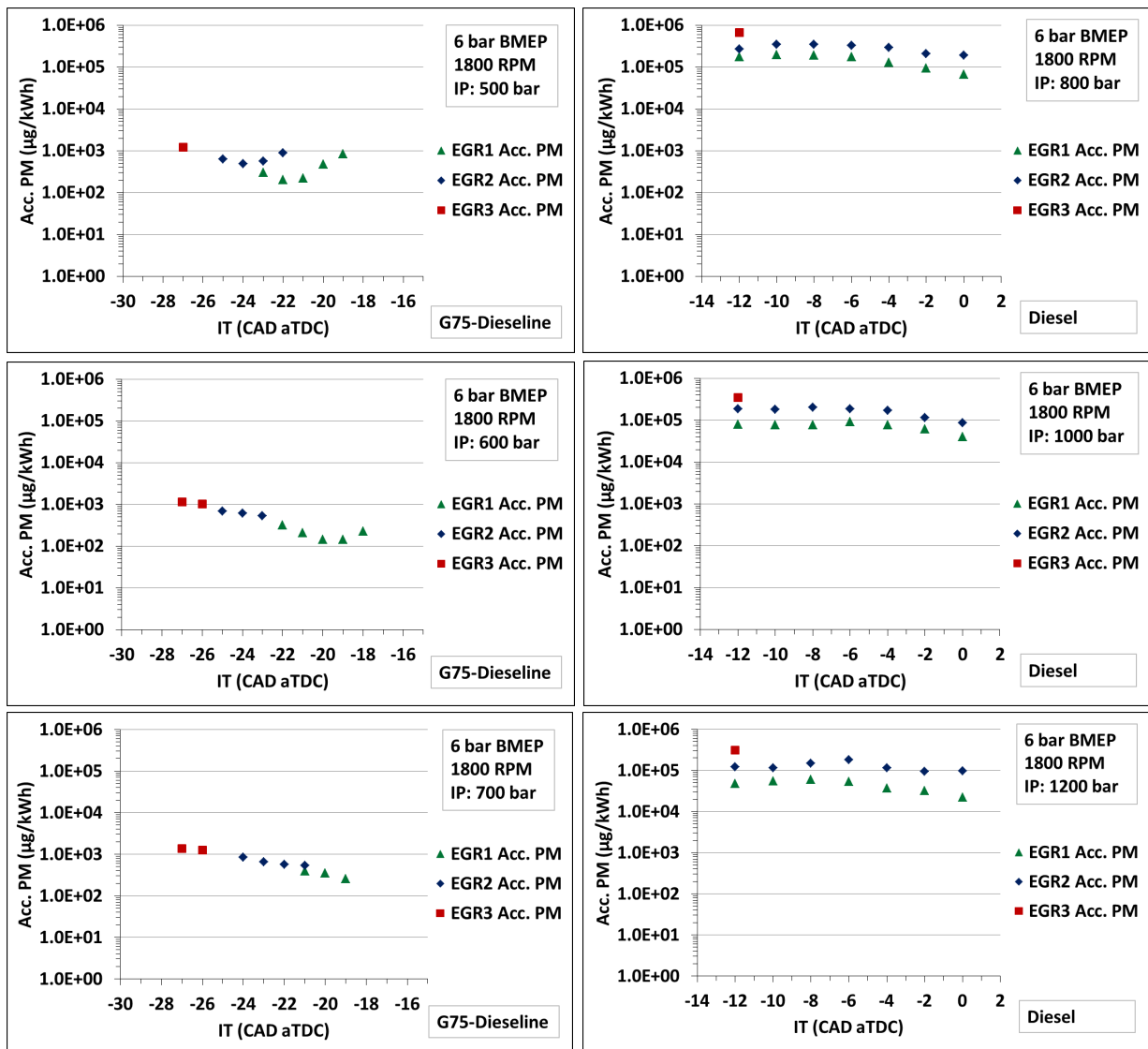
250 **Figure 4** Smoke emissions in terms of filter smoke number (FSN) for G75, left column, and diesel,
 251 right column, at different injection pressures, injection-timings and EGR valve positions at 6 bar
 252 BMEP (it should be noted that this graph is a semi-logarithmic plot)

253

254 In order to compare the mass of particle emissions from combustion of G75 and diesel fuels,
 255 brake specific accumulation mode particle mass (Acc. PM) emissions are illustrated in Figure
 256 5. Agglomerates are believed to be the main contributor to the mass of total emitted particles
 257 from an engine [29]. The variation trend of Acc. PM was similar to the variation trend of smoke
 258 for both of the fuels. For G75 fuel, most of the studied engine operating conditions at 6 bar
 259 BMEP resulted in Acc. PM of less than 0.001 g/kWh while for diesel they were between 0.023

260 to around 1 g/kWh. Therefore, this figure confirms that PM emissions from G75 combustion
 261 were less than diesel by orders of magnitude which is obviously beneficial even when an
 262 exhaust particulate filter is used.

263



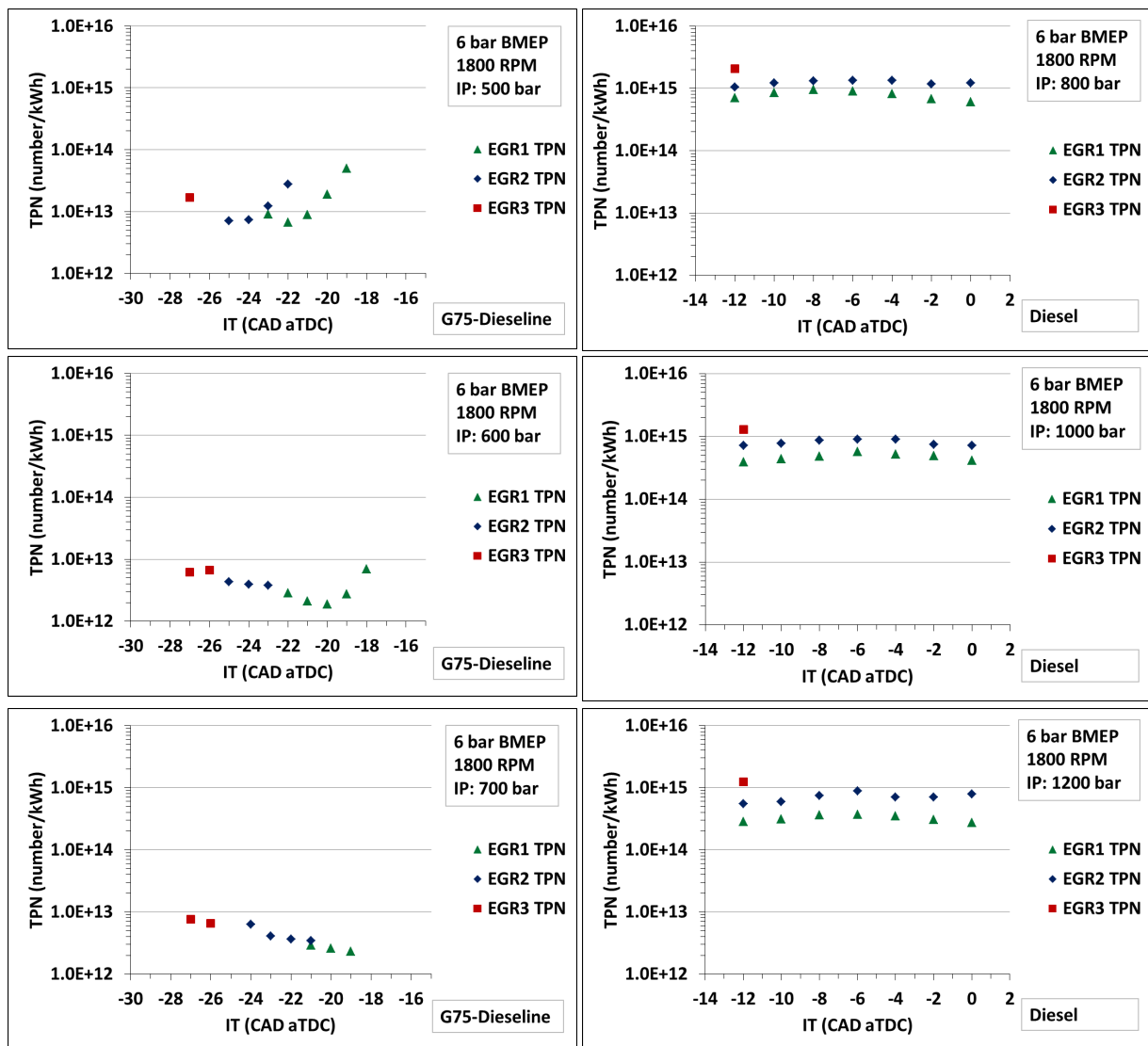
264

265 **Figure 5** Brake specific accumulation mode particle mass (Acc. PM) for G75, left column, and diesel,
 266 right column, at different injection pressures, injection-timings and EGR valve positions at 6 bar
 267 BMEP (it should be noted that this graph is a semi-logarithmic plot)

268

269 Brake specific total particle number (TPN) emissions are illustrated in Figure 6. These results
270 show the number of detected particles in the diameter range of 5 to 1000 nm in both nucleation
271 and accumulation modes. TPN emissions from G75 combustion were considerably lower than
272 diesel. Similar to the trend for PM, for diesel at a fixed IT, more EGR valve opening resulted
273 in higher TPN. This can be due to lower oxygen availability which results in more number of
274 locally rich fuel-air packets and weaker soot oxidation. In general, using higher IP for both of
275 the fuels resulted in lower TPN, probably due to better fuel and air mixing process. However,
276 this trend was not significant for particle mass emissions from G75 combustion. This
277 highlighted the necessity of investigating the size of these particles.

278



279

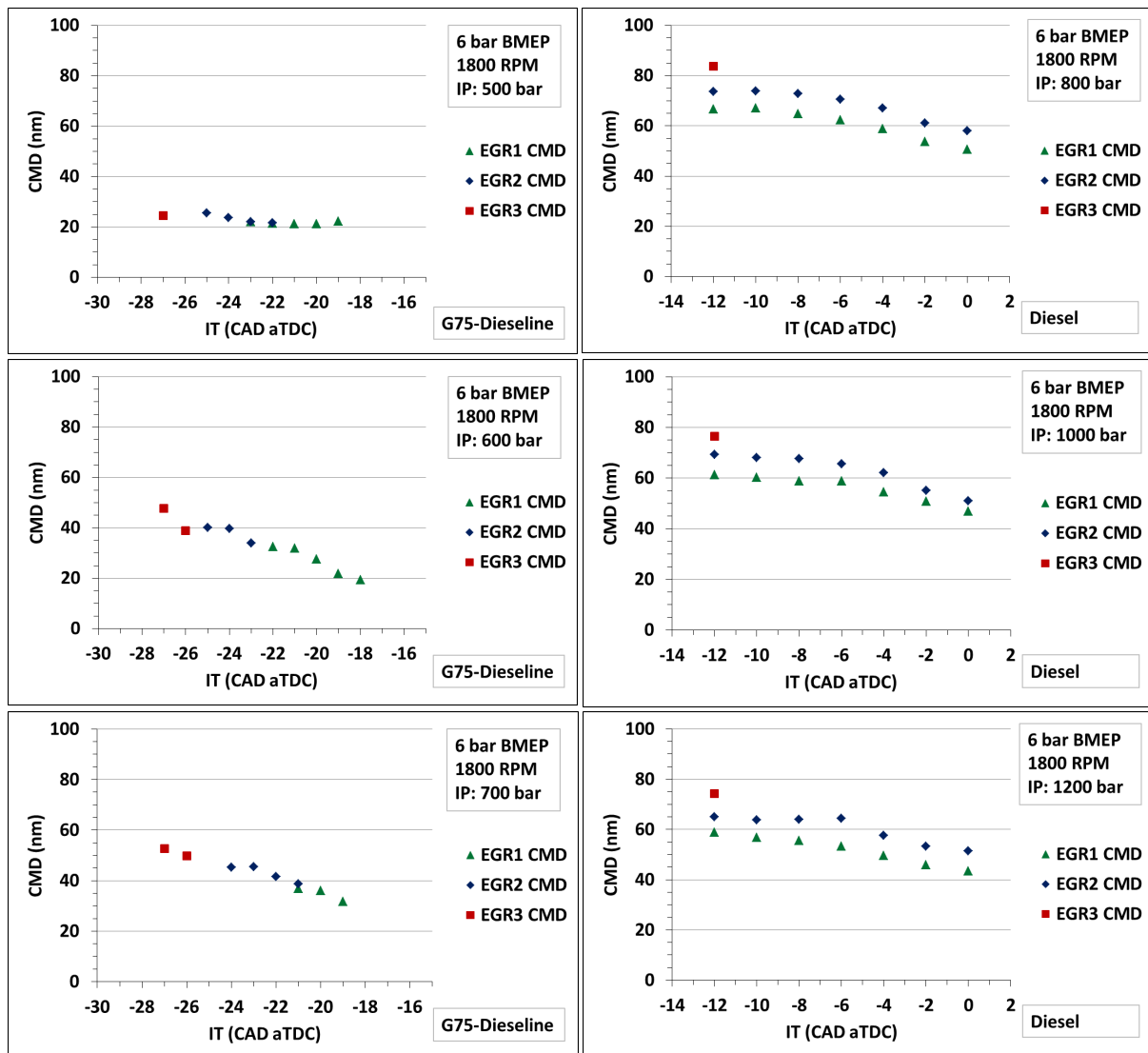
280 **Figure 6** Brake specific total particle number (TPN) for G75, left column, and diesel, right column, at
 281 different injection pressures, injection-timings and EGR valve positions at 6 bar BMEP (it should be
 282 noted that this graph is a semi-logarithmic plot)

283

284 Figure 7 shows the count median diameter (CMD) of particle emissions from G75 and diesel
 285 combustion. Based on these results, TPN values for G75 at the IP of 500 bar were dominated
 286 by smaller particles (total CMD is less than 30 nm) mainly in the nucleation mode. Using higher
 287 IPs of 600 and 700 bar for G75 resulted in larger total CMDs not because of the increased
 288 accumulation mode concentration but decrease in the PN mostly in the nucleation mode.
 289 Generally, diesel emissions, compared to G75 emissions, were dominated by larger diameter

290 particles as well as having higher nucleation and accumulation mode concentrations. For diesel,
 291 more EGR valve opening resulted in larger particles with CMD up to 83.7 nm indicating the
 292 dominance of larger agglomerates resulted from high equivalence-ratio of local fuel-air packets
 293 and possible lower rate of soot oxidation.

294



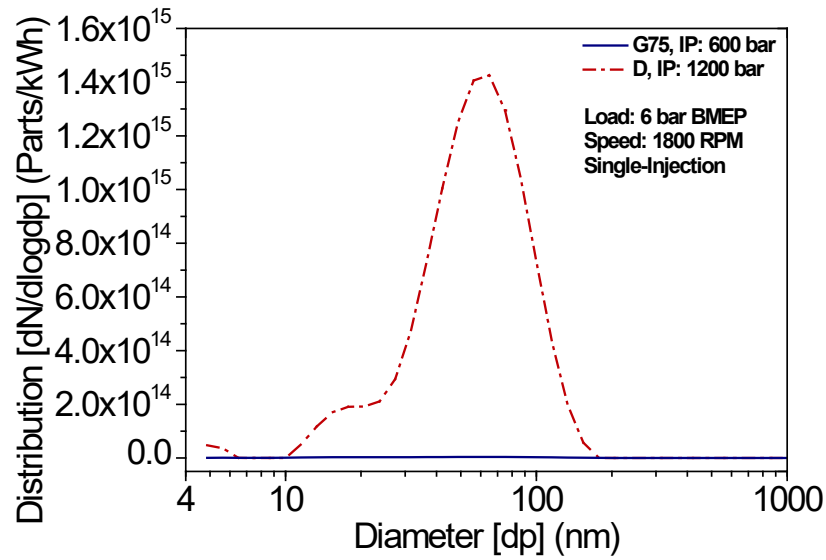
295

296 **Figure 7** Particles count median diameter (CMD) for G75, left column, and diesel, right column, at
 297 different injection pressures, injection-timings and EGR valve positions at 6 bar BMEP

298

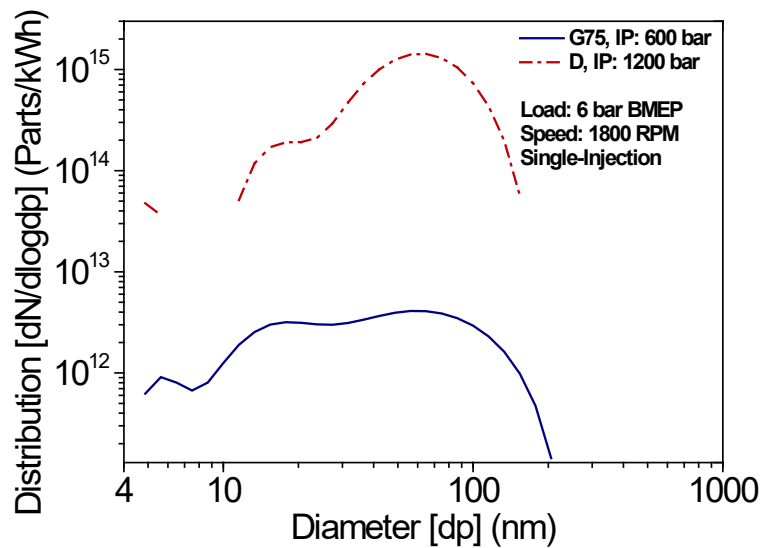
299 Figure 8 illustrates the brake specific particle size distribution comparing emissions of G75 and
300 diesel at two selected points.

301



303

(a)



305

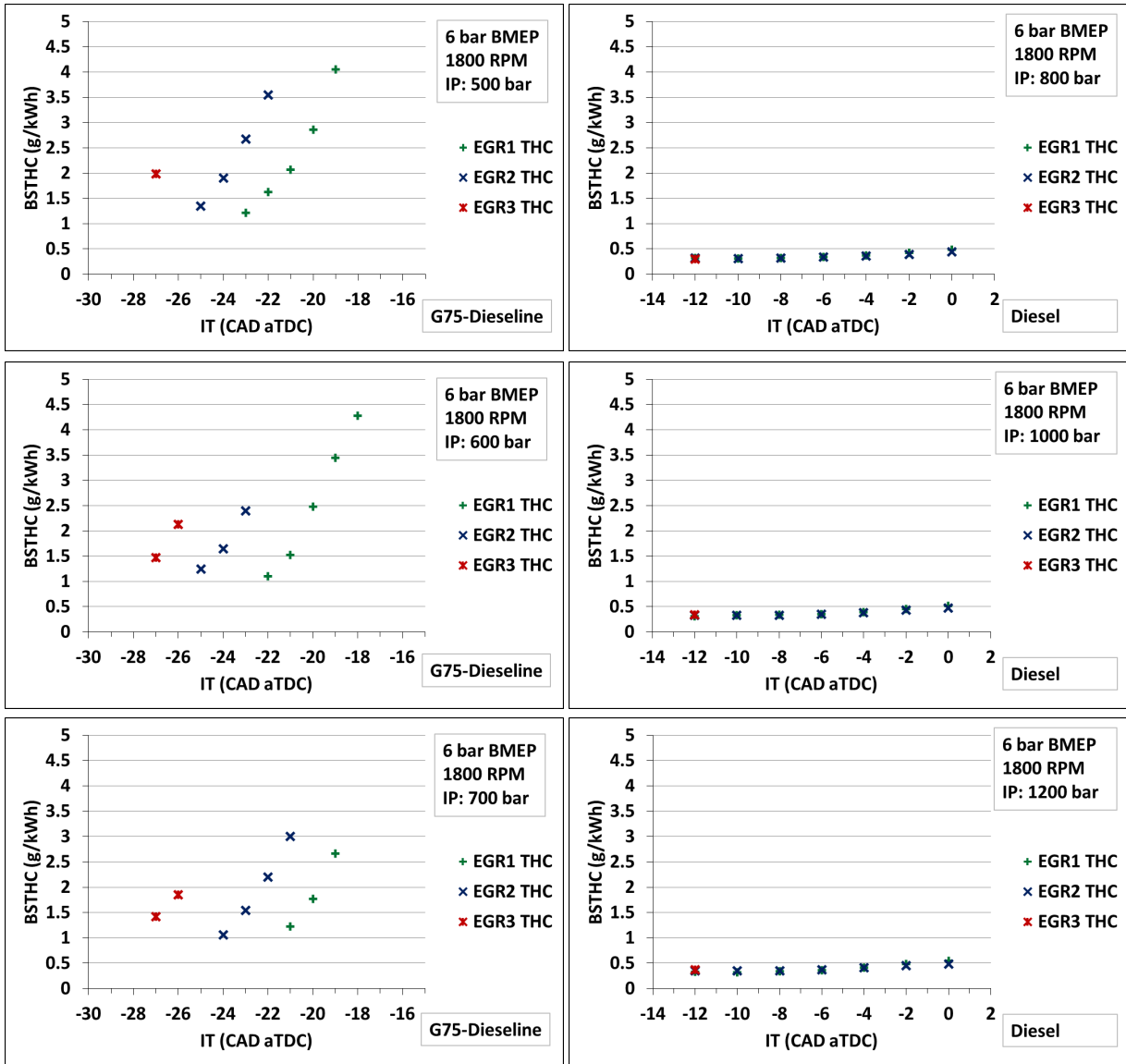
(b)

306 **Figure 8** Brake specific particle size distributions for G75 and diesel at 6 bar BMEP; (a) semi-
307 logarithmic plot and (b) log-log plot

308

309 These points were selected based on achieving minimum smoke and maximum BTE while
310 meeting the target of $BSNO_x < 0.4$ g/kWh. Settings for G75 were IP of 600 bar and IT of -24
311 CAD aTDC and for diesel were IP of 1200 bar and IT of -4 CAD aTDC with the EGR2 valve
312 setting for both. With these settings, diesel and G75 had almost the same BTE and $BSNO_x$
313 while smoke of diesel was 84 times more than smoke of G75 as shown in Figure 4. Compared
314 to diesel, Acc. BSPM and BSTPN emitted from G75 combustion were approximately 99.5%
315 lower. Based on Figure 8, particles emitted from diesel combustion were mainly in the
316 accumulation mode. No particles were detected in the size range of between approximately 6.5
317 nm and 10.0 nm. The small sub-6 nm tail in the results can be very small nuclei and their
318 concentration was very low compared to the detected particles in other size bins.
319 Concentrations of particles emitted from G75 combustion were lower than diesel in the entire
320 studied size range. The peaks associated with nucleation and accumulation mode particles were
321 in the same size range when comparing the two fuels, although at much lower concentrations
322 for G75. This can indicate that particle formation process was similar for both fuels but at a
323 much lower rate (especially for accumulation mode particles) and at different regions [3] for
324 low cetane-number fuels.

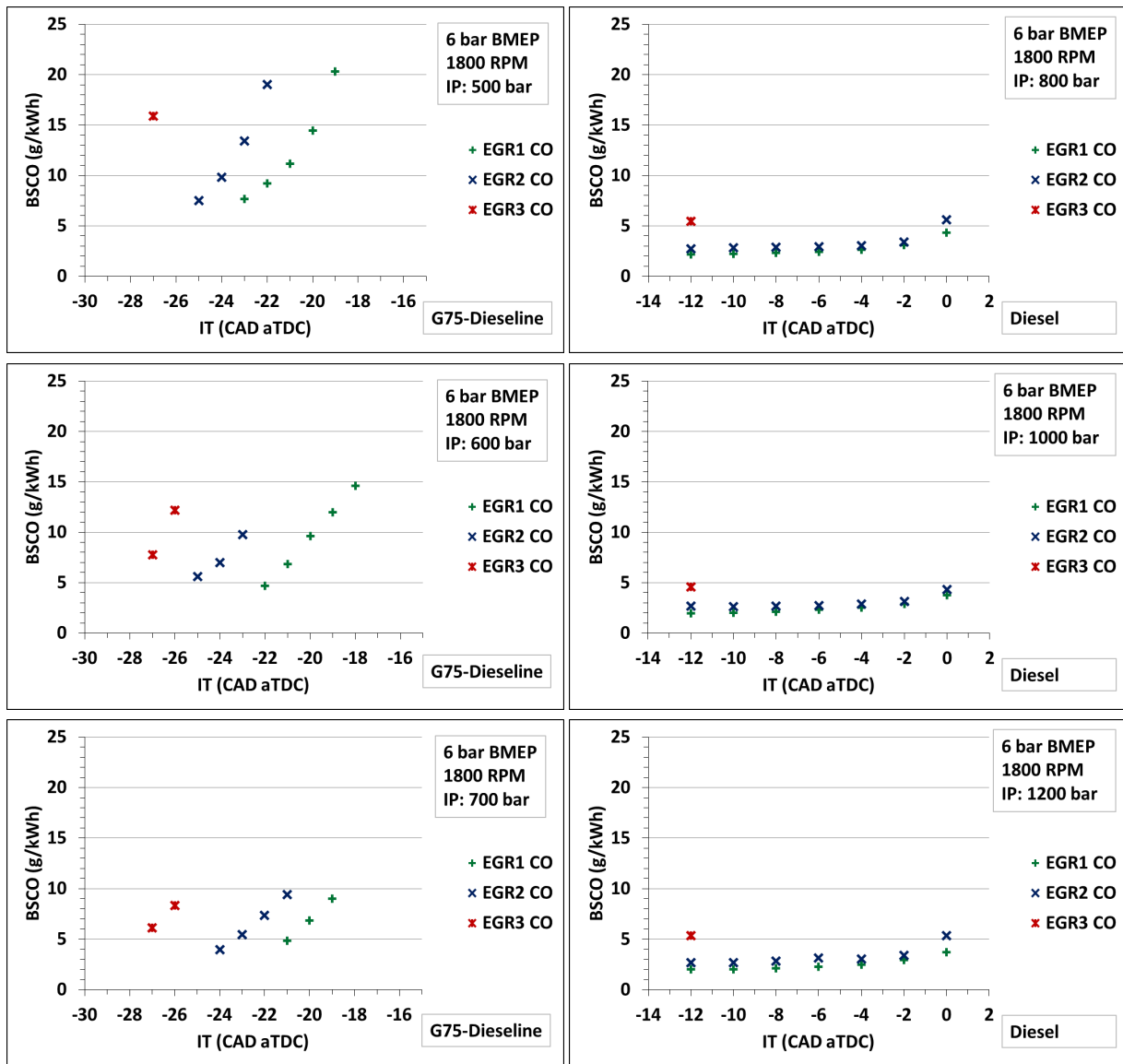
325 In general, compared to diesel combustion, G75 combustion resulted in higher BSTHC and
326 BSCO emissions as illustrated in Figure 9 and Figure 10, respectively. In contrast to the case
327 of G75 combustion, variations of BSTHC emissions from diesel combustion were not
328 significant and BSTHC stayed at less than approximately 0.5 g/kWh regardless of IP, EGR
329 valve opening and IT settings. Variations of BSCO emissions for diesel were also insignificant
330 compared to G75, although for both fuels more EGR valve opening increased BSCO slightly.
331 At the selected points discussed earlier, BSTHC and BSCO emissions of G75 was around 4
332 and 2.3 times higher than diesel, respectively, possibly due to fuel-air overmixing [3].



333

334 **Figure 9** Brake specific total hydrocarbons (BSTHC) for G75, left column, and diesel, right column,
 335 at different injection pressures, injection-timings and EGR valve positions at 6 bar BMEP

336



337

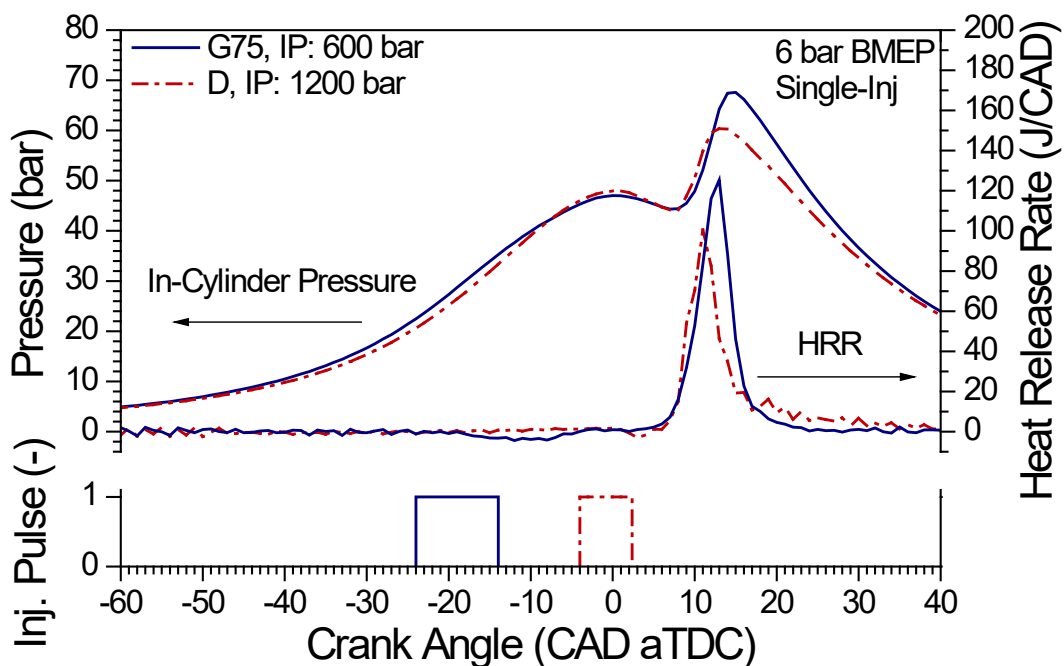
338 **Figure 10** Brake specific carbon monoxide (BSCO) for G75, left column, and diesel, right column, at
 339 different injection pressures, injection-timings and EGR valve positions at 6 bar BMEP

340

341 Figure 11 illustrates in-cylinder pressure, heat release rate (HRR) and injection pulse of G75
 342 and diesel at two selected points (similar to what was discussed earlier for minimum smoke
 343 and maximum BTE). These points had the same AHR-50 fixed at 12 CAD aTDC. The reason
 344 for shorter pulse duration for diesel fuel is the fact that it was injected at a higher pressure
 345 compared to G75. It can be seen that the separation between the end of injection (EOI) and the
 346 start of combustion (SOC) for G75 was more pronounced compared to diesel owing to its

347 longer ignition-delay at this load. This supports better fuel-air mixing and consequently lower
 348 particle emissions. G75 combustion resulted in a higher peak of HRR and in-cylinder pressure
 349 compared to diesel due to more premixed combustion. There were some slight differences in
 350 the in-cylinder pressure trace of G75 and diesel during the later stages of compression stroke
 351 (Figure 11). Different in-cylinder gas temperature history, in-cylinder gas composition and
 352 combustion mode for G75 and diesel can be hypothesised to have caused these relatively small
 353 differences at this engine load. After the start of G75 injection, there was a reduction of HRR
 354 probably due to the cooling effect of fuel. This cooling effect reduced the top dead centre peak
 355 pressure compared to diesel which was injected closer to the TDC.

356



357

358 **Figure 11** In-cylinder pressure, heat release rate and injection pulse for G75 and diesel at 6 bar BMEP
 359 using single-injection

360

361 Based on the results presented for 6 bar BMEP using single-injection, changes in combustion
 362 and emissions characteristics of G75 when varying the IT were more significant compared to

363 diesel. This indicates the importance of the AHR-50 for G75 fuel due to its longer ignition-
364 delay. There was a trade-off between THC-CO reduction and NO_x reduction when operating
365 on G75. The main issue for diesel combustion at this load was high smoke emissions which
366 can be reduced at the expense of either increased BSNO_x or reduced BTE. For both fuels there
367 was a trade-off between increasing BTE and decreasing NO_x.

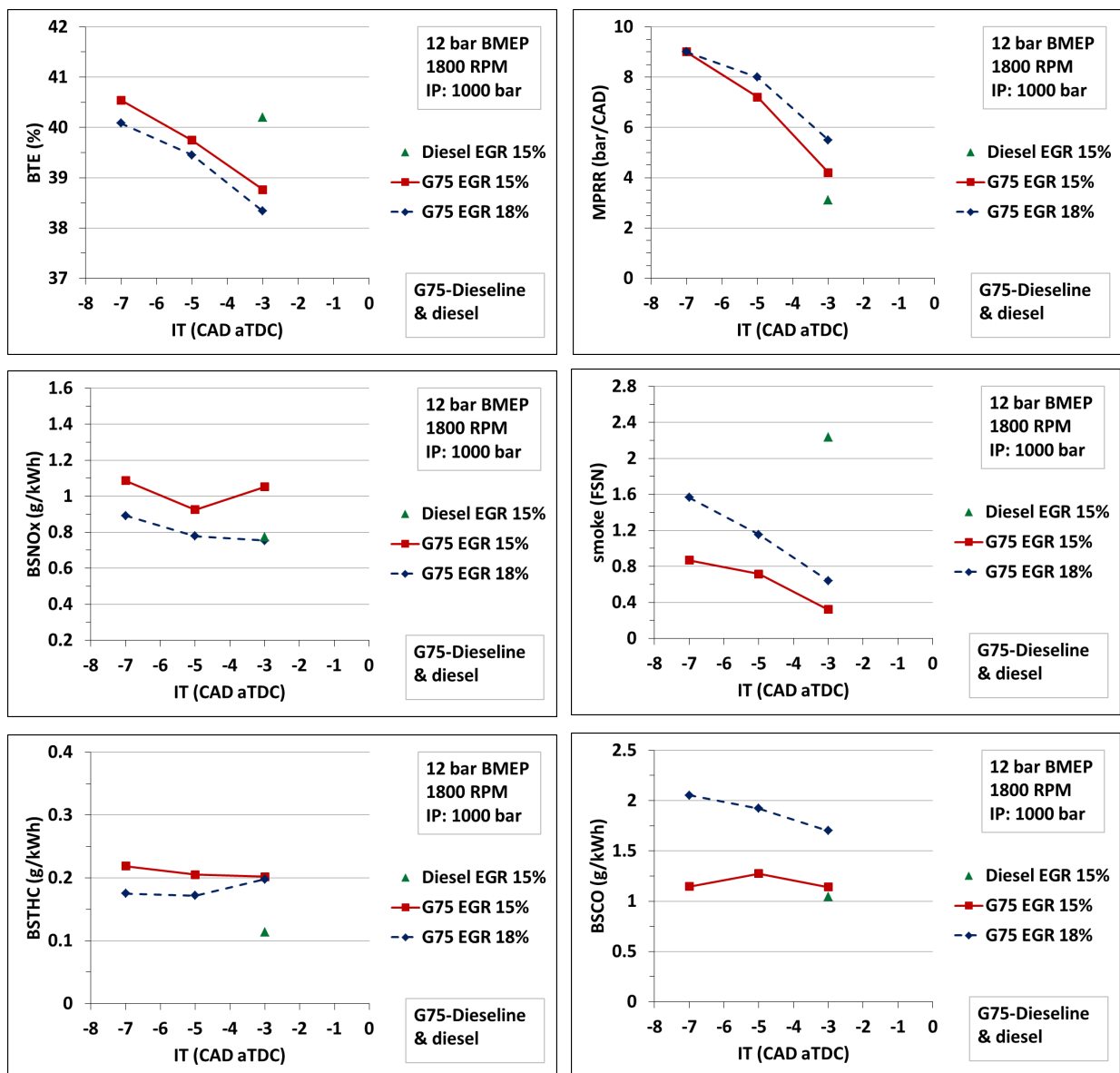
368 **3.2. Results at 12 bar BMEP**

369 Longer ignition-delay (ID) of G75, compared to diesel, observed at lower loads was less
370 significant at 12 bar BMEP due to higher in-cylinder pressure and temperature. Screening tests
371 at 12 bar BMEP with G75 indicated that there were difficulties with achieving low-NO_x and
372 low-smoke combustion. It was concluded that λ had to be always more than 1.2; otherwise
373 smoke emissions were more than 3 FSN and combustion was unstable for G75. Dependence
374 of smoke emissions on this λ limit had consequences for BSNO_x emissions. Using high rates
375 of EGR in order to decrease BSNO_x, lowered λ and consequently higher intake pressure was
376 required to compensate for the reduced intake O₂ which was a challenge for the VNT
377 turbocharger. Moreover, producing more intake pressure using the turbocharger means more
378 backpressure for the engine and therefore more pumping losses.

379 Figure 12 illustrates the results for single-injection of G75 with the IP of 1000 bar at two EGR
380 rates, 15% and 18% (while λ was fixed between 1.2 and 1.3), and three different ITs. Using
381 IPs below 1000 bar resulted in high smoke values (more than 3 FSN). In this figure, there is
382 also a base case for diesel single-injection with the same IP for comparison purposes. BTE of
383 G75 combustion at this load was increased by advancing the IT at both rates of EGR. This was
384 due to occurrence of combustion closer to the TDC (advanced AHR-50) which increased BTE
385 as well as MPRR. Smoke emissions followed the same trend in response to advancing the IT
386 and higher EGR rate resulted in elevated smoke emissions as opposed to the observations at 6

387 bar BMEP. This can be linked with combustion temperature, O₂ availability and possible fuel
 388 spray-piston interaction. Differences in BSTHC and BSCO emissions from combustion of G75
 389 and diesel were insignificant as shown in Figure 12. These results indicate that G75 emissions
 390 were more similar to diesel as opposed to the observations at the lower studied load, although
 391 smoke emissions were still lower.

392

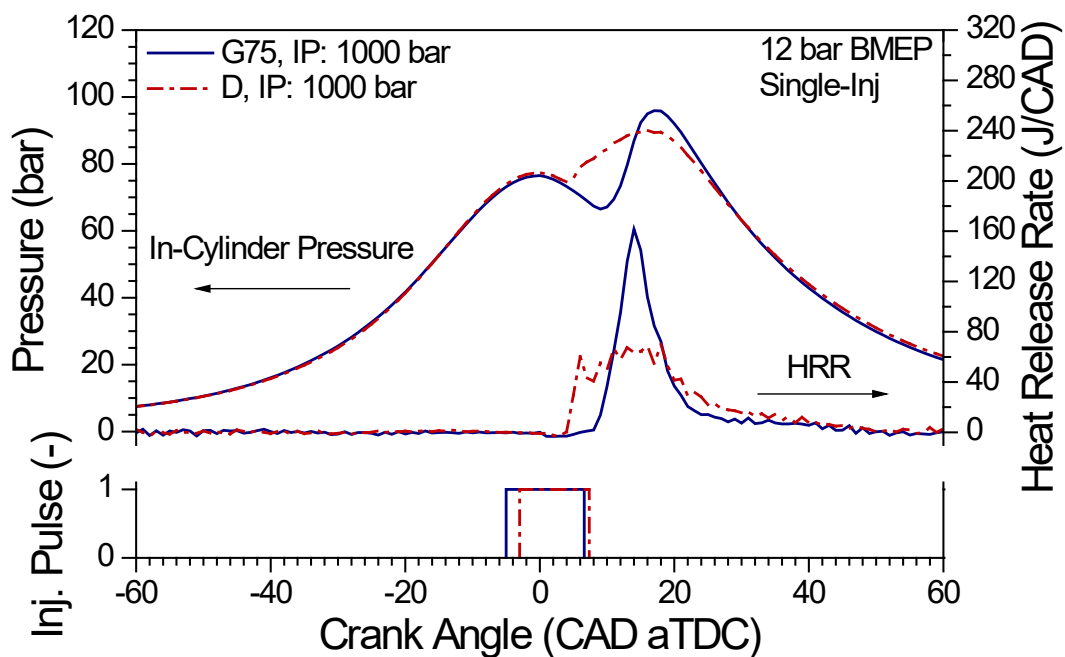


393

394 **Figure 12** Comparison of results of G75 with the results of baseline diesel at 12 bar BMEP with fixed
 395 injection pressure of 1000 bar

396 In-cylinder pressure, HRR and injection pulse of G75 were compared to diesel at the same IP,
 397 EGR rate and combustion-phasing (Figure 13). Using diesel resulted in mixing-controlled
 398 combustion indicated by the negative ignition-dwell and low peak of HRR. G75 combustion
 399 was more close to the premixed type combustion with a relatively longer ID, although ignition-
 400 dwell was not significantly long. The main outcome of the difference between combustion of
 401 these two fuels was the higher smoke emission of diesel shown in Figure 12. From these results,
 402 clearly MPRR for G75 combustion was higher than diesel at the same AHR-50, although it
 403 was <10 bar/CAD.

404



405

406 **Figure 13** In-cylinder pressure, heat release rate and injection pulse for G75 and diesel at 12 bar
 407 BMEP, IP of 1000 bar and EGR rate of 15%

408

409 Increasing IP from 1000 to 1200 bar for both fuels, with fixed λ and AHR-50 at 1.2 and 13
 410 CAD aTDC, respectively, resulted in reduced BTE (Table 3). This can be due to more
 411 mechanical load on the engine when using a higher IP. While BTE of both fuels was in the

412 same range, smoke emission of diesel combustion was higher than G75 by around 3.35 times.
 413 However, BSNO_x emission of G75 was around 1.6 times more than the results for diesel. This
 414 means at this load, there was a trade-off between NO_x and smoke reduction for both of the
 415 studied fuels.

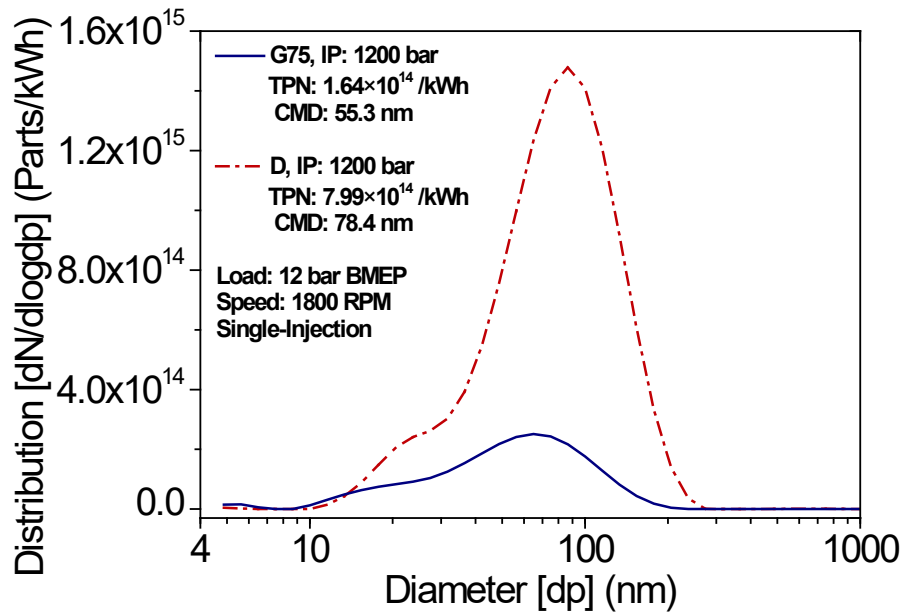
416 Brake specific particle number and size distributions are presented in Figure 14. G75 fuel
 417 combustion resulted in less TPN (by around 79.5%) while total CMD was 23.1 nm smaller
 418 compared to diesel combustion. Normalised concentrations of particles for G75 (in terms of
 419 Parts/kWh) were higher in this load compared to the lower loads. Similar to the results at 6 bar
 420 BMEP, bimodal distributions were observed for both fuels while concentrations of particles
 421 emitted from G75 combustion were lower than diesel in most of the studied size bins.
 422 Accumulation mode concentration peaked at a smaller particle diameter for G75 compared to
 423 diesel. It can be hypothesised that this was mainly due to better fuel-air mixing process.

424

425 **Table 3** Comparison of G75 and diesel at 12 bar BMEP with fixed injection pressure and combustion-
 426 phasing; IT for G75 and diesel were -5 and -3 CAD aTDC, respectively

Fuel	IP	BTE	BSNO_x	BSTHC	BSCO	smoke
(-)	bar	%	g/kWh	g/kWh	g/kWh	FSN
G75	1200	39.53	1.01	0.15	1.43	0.819
Diesel	1200	39.78	0.63	0.08	1.40	2.744

427



428

429 **Figure 14** Brake specific particle number and size distribution for G75 and diesel at 12 bar BMEP

430

431 3.3. Results at 17.3 bar BMEP

432 Results at the high load of 17.3 bar BMEP showed similar trends to the results at 12 bar BMEP
 433 for G75 fuel combustion (Table 4). When operating on G75 fuel, IPs above 1100 bar could not
 434 be achieved. It can be hypothesised that some properties of G75 fuel, most importantly lower
 435 viscosity and initial boiling point, could have some effects on the operation of the high pressure
 436 fuel pump.

437 Increase of the EGR rate and retarding the IT reduced BTE and BSNO_x but increased smoke.
 438 However, at 12 bar BMEP, smoke was reduced as IT was retarded. This can be explained by
 439 considering the possible differences in the rate of soot generation and soot oxidation at these
 440 two loads. Earlier ITs resulted in longer IDs, although for the entire studied cases ignition-
 441 dwell was negative. It should be mentioned that absolute intake pressure at this load was more
 442 than 2.5 bar and therefore ID was shorter [30].

443 **Table 4** G75 combustion performance and emissions results at 17.3 bar BMEP and IP of 1100 bar

IT	EGR	BTE	BSNO _x	BSTHC	BSCO	smoke	TPN	Acc. PM
CAD aTDC	%	%	g/kWh	g/kWh	g/kWh	FSN	Number/kWh	g/kWh
-3	4.79	39.25	2.46	0.14	1.02	0.935	2.08×10 ¹⁴	0.068
-3	5.46	39.04	2.11	0.09	0.96	1.024	2.02×10 ¹⁴	0.074
-1	5.02	37.77	1.76	0.07	1.60	2.144	3.15×10 ¹⁴	0.130

444

445 Results of the G75 combustion were compared to results of the diesel combustion (listed in
 446 Table 5) with the same AHR-50 and EGR rate (4.7%). Compared to diesel results, using G75
 447 reduced smoke and TPN emissions by approximately 44.7% and 46.9%, respectively, while
 448 BSNO_x emissions were higher by approximately 1.43 times. This is possibly due to more
 449 pronounced premixed portion of the G75 combustion as a result of its relatively longer ID
 450 compared to diesel. Similar to 12 bar BMEP, increasing the EGR rate was limited by the
 451 available intake pressure from the VNT turbocharger. It seems that properties of G75 fuel were
 452 not significantly helpful to reduce NO_x and smoke simultaneously at this high load in the
 453 current engine. The mixing-controlled nature of the combustion for both fuels resulted in
 454 observing the trade-off for NO_x and soot reduction.

455

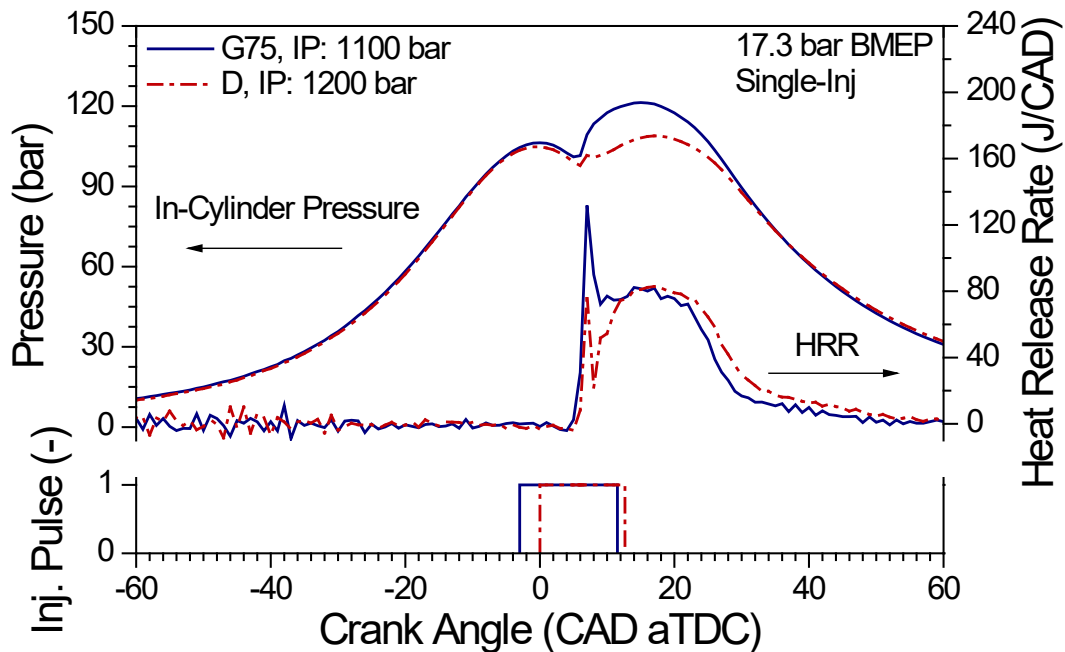
456 **Table 5** Comparison of G75 and diesel at 17.3 bar BMEP with the same AHR-50; IT of G75 and
 457 diesel were fixed at -3 and 0 CAD aTDC, respectively

Fuel	IP	BTE	BSNO _x	BSTHC	BSCO	smoke	TPN	Acc. PM
(-)	bar	%	g/kWh	g/kWh	g/kWh	FSN	Number/kWh	g/kWh
G75	1100	39.25	2.46	0.14	1.02	0.935	2.08×10 ¹⁴	0.068
Diesel	1200	38.96	1.72	0.06	0.95	1.692	3.92×10 ¹⁴	0.146

458

459 Figure 15 illustrates in-cylinder pressure, HRR and injection pulse for both fuels at 17.3 bar
 460 BMEP with settings used in Table 5. SOC for both fuels was before the EOI resulting in a
 461 lower peak of HRR compared to 12 bar BMEP as less premixing was achieved.

462



463

464 **Figure 15** In-cylinder pressure, heat release rate and injection pulse for G75 and diesel at 17.3 bar
 465 BMEP

466

467 It can be concluded that G75 and diesel fuels illustrated similar combustion and emissions
 468 characteristics at high loads. It is suggested that, for high loads, higher intake pressure should
 469 be investigated while considering effects of the imposed higher backpressure on engine
 470 efficiency. It is expected that with higher intake pressure, more EGR can be used and therefore
 471 NO_x will be reduced while intake O_2 concentration is high enough to either reduce soot
 472 formation or improve soot oxidation [3, 28, 31, 32]. Moreover, interactions between the fuel
 473 spray and piston and/or cylinder walls need to be studied for G75. Hole diameter and included
 474 angle of the injector as well as the geometry of piston and cylinder head are required to be

475 optimised to suit G75 fuel and its combustion. Optimisation of the fuel injection and EGR
476 strategies for G75 combustion can be another area of development. Furthermore, since
477 combustion of G75 and diesel is more similar at high loads, there is a scope for studying fuel
478 composition effects, e.g HC structure, aromatics content and oxygenates content, on particle
479 emissions [31, 33]. Addition of viscosity improver to the G75 can be investigated to identify
480 any improvements on achieving higher injection pressures at high loads.

481

482 **4 SUMMARY AND CONCLUSIONS**

483 Compression ignition (CI) combustion of G75-Dieseline (G75) and diesel in a light-duty 4-
484 cylinder engine has been investigated at a fixed engine speed of 1800 RPM and at 6, 12 and
485 17.3 bar BMEP. The major findings are as follows:

- 486 • Particle emissions from G75 combustion were lower than diesel combustion by up to
487 99.5% in both number and mass, while BTE and NO_x remained in the same range. This
488 was mainly due to the longer ignition-delay and higher volatility of G75.
- 489 • Bimodal particle size distributions (nucleation and accumulation modes) were observed
490 for both fuels while particle concentrations (especially accumulation mode) for G75
491 were much lower at the entire particle size range.
- 492 • The reduction of particle number emissions caused by increasing the fuel injection
493 pressure was less evident in the accumulation mode compared to the nucleation mode
494 for G75. The variation trend of particle mass emissions was similar to smoke.
- 495 • At medium loads, premixed combustion and emissions of G75 were more sensitive to
496 the fuel injection timing compared to diesel due to its longer ignition-delay and ignition-
497 dwell.

498 • At high loads (especially 17.3 bar BMEP in this study), the mixing-controlled
499 combustion following the phase of premixed combustion was observed for G75,
500 although less pronounced than in diesel combustion, because of shorter ignition-delay
501 compared to lower loads.

502 There is a scope for optimising the intake pressure boosting system, piston/cylinder-head
503 geometries, injector included angle and fuel injection strategies for G75 combustion. These
504 will be helpful for further reduction of NO_x and smoke emissions at high operating loads.

505

506 **ACKNOWLEDGEMENTS**

507 Special appreciations go to Jaguar Land Rover and Shell for their generous support and
508 contribution to our on-going research in the University of Birmingham. The authors would like
509 to thank Professor Gautam Kalghatgi for his invaluable scientific discussions and comments.
510 Thanks go to technicians at the University of Birmingham, Mr. Carl Hingley, Mr. Rickie
511 Creegan, Mr. Peter Thornton, Mr. Jack Garrod and Mr. Lee Gauntlett for their help with setting
512 up the engine test cell. Support of project NFSC 51636003 (China) is acknowledged.

513

514 REFERENCES

- 515 [1] Kalghatgi G. Fuel/Engine Interactions. SAE International; 2013.
- 516 [2] Kalghatgi G, Hildingsson L, Johansson B. Low NOx and Low Smoke Operation of a
517 Diesel Engine Using Gasolinelike Fuels. *Journal of Engineering for Gas Turbines and*
518 *Power* 2010;132(9):092803-.
- 519 [3] Musculus MPB, Miles PC, Pickett LM. Conceptual models for partially premixed
520 low-temperature diesel combustion. *Progress in Energy and Combustion Science*
521 2013;39(2-3):246-83.
- 522 [4] Benajes J, Novella R, Garcia A, Domenech V, Durrett R. An Investigation on Mixing
523 and Auto-ignition using Diesel and Gasoline in a Direct-Injection Compression-
524 Ignition Engine Operating in PCCI Combustion Conditions. *SAE Int J Engines*
525 2011;4(2):2590-602.
- 526 [5] Zhang F, Zeraati Rezaei S, Xu H, Shuai S-J. Experimental Investigation of Different
527 Blends of Diesel and Gasoline (Dieseline) in a CI Engine. *SAE International Journal*
528 *of Engines* 2014;7(4):1920-30.
- 529 [6] Zeraati Rezaei S, Zhang F, Xu H, Ghafourian A, Herreros JM, Shuai S. Investigation
530 of two-stage split-injection strategies for a Dieseline fuelled PPCI engine. *Fuel*
531 2013;107:299-308.
- 532 [7] Zeraati-Rezaei S, Al-Qahtani Y, Xu H. Investigation of hot-EGR and low pressure
533 injection strategy for a Dieseline fuelled PCI engine. *Fuel* 2017;207:165-78.
- 534 [8] Kalghatgi GT, Hildingsson L, Harrison AJ, Johansson B. Surrogate fuels for
535 premixed combustion in compression ignition engines. *International Journal of*
536 *Engine Research* 2011;12(5):452-65.
- 537 [9] Kalghatgi G, Johansson B. Gasoline compression ignition approach to efficient, clean
538 and affordable future engines. *Proceedings of the Institution of Mechanical Engineers,*
539 *Part D: Journal of Automobile Engineering* 2017:0954407017694275.
- 540 [10] Algunaibet IM, Voice AK, Kalghatgi GT, Babiker H. Flammability and volatility
541 attributes of binary mixtures of some practical multi-component fuels. *Fuel*
542 2016;172:273-83.
- 543 [11] Burger JL, Gough RV, Bruno TJ. Characterization of Dieseline with the Advanced
544 Distillation Curve Method: Hydrocarbon Classification and Enthalpy of Combustion.
545 *Energy & Fuels* 2013;27(2):787-95.
- 546 [12] Zhang F, Xu H, Zhang J, Tian G, Kalghatgi G. Investigation into Light Duty
547 Dieseline Fuelled Partially-Premixed Compression Ignition Engine. *SAE International*
548 *Journal of Engines* 2011;4(1):2124-34.
- 549 [13] Zhang F. Spray, combustion and emission characteristics of dieseline fuel. Ph.D.: PhD
550 Thesis, University of Birmingham; 2013.
- 551 [14] Turner D, Tian G, Xu H, Wyszynski ML, Theodoridis E. An Experimental Study of
552 Dieseline Combustion in a Direct Injection Engine. SAE International, SAE Technical
553 Paper 2009-01-1101; 2009.
- 554 [15] Wang J, Wang Z, Liu H. Combustion and emission characteristics of direct injection
555 compression ignition engine fueled with Full Distillation Fuel (FDF). *Fuel*
556 2015;140:561-7.
- 557 [16] Liu H, Wang Z, Wang J, He X. Effects of gasoline research octane number on
558 premixed low-temperature combustion of wide distillation fuel by gasoline/diesel
559 blend. *Fuel* 2014;134:381-8.

- 560 [17] Zhang F, Xu H, Zeraati Rezaei S, Kalghatgi G, Shuai S-J. Combustion and Emission
561 Characteristics of a PPCI Engine Fuelled with Dieseline. SAE International, SAE
562 Technical Paper 2012-01-1138; 2012.
- 563 [18] Wei M, Li S, Xiao H, Guo G. Combustion performance and pollutant emissions
564 analysis using diesel/gasoline/iso-butanol blends in a diesel engine. Energy
565 Conversion and Management 2017;149:381-91.
- 566 [19] Belgiorno G, Di Blasio G, Shamun S, Beatrice C, Tunestål P, Tunér M. Performance
567 and emissions of diesel-gasoline-ethanol blends in a light duty compression ignition
568 engine. Fuel 2018;217:78-90.
- 569 [20] Benajes J, García A, Monsalve-Serrano J, Boronat V. Gaseous emissions and particle
570 size distribution of dual-mode dual-fuel diesel-gasoline concept from low to full load.
571 Applied Thermal Engineering 2017;120:138-49.
- 572 [21] Benajes J, García A, Monsalve-Serrano J, Boronat V. An investigation on the
573 particulate number and size distributions over the whole engine map from an
574 optimized combustion strategy combining RCCI and dual-fuel diesel-gasoline.
575 Energy Conversion and Management 2017;140:98-108.
- 576 [22] Reitz RD, Duraisamy G. Review of high efficiency and clean reactivity controlled
577 compression ignition (RCCI) combustion in internal combustion engines. Progress in
578 Energy and Combustion Science 2015;46:12-71.
- 579 [23] Heywood JB. Internal combustion engine fundamentals. McGraw-Hill; 1988.
- 580 [24] CAMBUSTION. DMS500 Fast Particulate Analyzer - User Manual - Version 4.03.
581 2015.
- 582 [25] CAMBUSTION. Combustion Application Note DMS06 - Real-time Mode Finding &
583 Lognormal Fitting with DMS Series Fast Particulate Spectrometers; 2015. Available
584 from:
585 <http://www.cambustion.com/sites/default/files/applications/DMS/dms06v03.pdf>.
586 [Accessed 16/02/2017 2017].
- 587 [26] CAMBUSTION. Combustion Application Note DMS01 - Particulate Mass
588 Measurement with DMS Series Fast Spectrometers; 2015. Available from:
589 <http://www.cambustion.com/sites/default/files/applications/DMS/dms01v05.pdf>.
590 [Accessed 30/07/2016 2016].
- 591 [27] Yanowitz J, Ratcliff MA, McCormick RL, Taylor JD, Murphy MJ. Compendium of
592 Experimental Cetane Numbers. ; National Renewable Energy Lab. (NREL), Golden,
593 CO (United States); 2017:Medium: ED; Size: 78 p.
- 594 [28] Ladommatos N, Abdelhalim S, Zhao H. The effects of exhaust gas recirculation on
595 diesel combustion and emissions. International Journal of Engine Research
596 2000;1(1):107-26.
- 597 [29] Kittelson DB. Engines and nanoparticles: a review. Journal of Aerosol Science
598 1998;29(5-6):575-88.
- 599 [30] Dec JE, Yang Y, Dernote J, Ji C. Effects of Gasoline Reactivity and Ethanol Content
600 on Boosted, Premixed and Partially Stratified Low-Temperature Gasoline
601 Combustion (LTGC). SAE International Journal of Engines 2015;8(3).
- 602 [31] Eastwood P. Particulate emissions from vehicles. SAE International and Wiley-
603 PEPublishing Series; 2008.
- 604 [32] Dec JE. A Conceptual Model of DI Diesel Combustion Based on Laser-Sheet
605 Imaging*. SAE International, SAE Technical Paper 970873; 1997.
- 606 [33] Ladommatos N, Rubenstein P, Bennett P. Some effects of molecular structure of
607 single hydrocarbons on sooting tendency. Fuel 1996;75(2):114-24.

608

609 **APPENDIX**

610 **Nomenclature**

Acc. PM	Accumulation mode particle mass
AHR-50	Combustion-phasing (defined as the CAD at which 50% of the accumulative heat release is achieved)
aTDC	After top dead centre
BMEP	Brake mean effective pressure
BS	Brake specific
BTE	Brake thermal efficiency
CAD	Crank angle degree
CI	Compression ignition
CMD	Count median diameter
CN	Cetane-number
CO	Carbon monoxide
CO ₂	Carbon dioxide
DAQ	Data acquisition board
DI	Direct injection
Dieseline	A blend of diesel and gasoline
ECU	Engine control unit
EGR	Exhaust gas recirculation
EOI	End of injection
FSN	Filter smoke number
G75	A blend of 75% gasoline in diesel based on volume
HC	Hydrocarbons

HRR	Heat release rate
ID	Ignition-delay
IP	Injection pressure
IT	Injection-timing
MPRR	Maximum pressure rise rate
NO _x	Oxides of nitrogen
O ₂	Oxygen
PCI	Premixed compression ignition
RON	Research octane number
RPM	Revolutions per minute
SD	Standard deviation
SOC	Start of combustion
TDC	Top dead centre
THC	Total hydrocarbons
TPN	Total particle number
VNT	Variable-nozzle-turbine
λ	Specific air-fuel ratio (actual air/fuel ratio over stoichiometric air/fuel ratio)